Ethanol conversion into 1,3-butadiene over a mixed Hf-Zn catalyst: effect of reaction conditions and water content in ethanol

G. M. Cabello González[1], P. Concepción[2], A. L. Villanueva Perales*[1], A. Martínez[2], M. Campoy[1], F. Vidal-Barrero[1]

[1] Departamento de Ingeniería Química y Ambiental, Escuela Técnica Superior de Ingeniería, Universidad de Sevilla, Camino de los Descubrimientos, s/n. 41092 Sevilla, Spain.

[2] Instituto de Tecnología Química, Universitat Politècnica de València-Consejo Superior de Investigaciones Científicas (UPV-CSIC), Avda. de los Naranjos s/n, 46022 Valencia, Spain.

* Corresponding author

Email: angelluisvp@us.es

Departamento de Ingeniería Química y Ambiental, Escuela Técnica Superior de Ingeniería, Universidad de Sevilla, Camino de los Descubrimientos, s/n. 41092 Sevilla, Spain.

Abstract

Assessment of catalyst performance is necessary for process design in order to evaluate the effect of reaction conditions on process economics and configuration. In this work, the combined effect of reaction conditions and quality of feedstock (i.e. water content) on the performance of a Hf-Zn catalyst, prepared by physically mixing the zinc silicate hemimorphite and HfO_2/SiO_2, for the conversion of ethanol to 1,3-butadiene is investigated. To this aim, an experimental design was performed with temperature, space velocity, and water content in ethanol as factors. In situ IR spectroscopy unambiguously indicates that the presence of water in the ethanol feed induces the generation of new Brønsted acid sites, most probably by reaction of Zn^{2+}-related Lewis acid sites with water, and thus modifies the Brønsted-Lewis acid site balance in the catalyst. This fact results in (i) higher selectivity to dehydration products catalyzed by Brønsted acid sites, and (ii) lower ethanol conversion as some Zn^{2+} Lewis acid sites, active for the dehydrogenation of ethanol, are transformed into Brønsted acid sites. In addition, higher acetaldehyde yield is observed in experiments feeding hydrous ethanol, indicating that water inhibits aldol condensation reactions to a larger degree than ethanol dehydrogenation. This effect is particularly beneficial at a high operating temperature, where acetaldehyde is so reactive that it is rapidly converted to heavy compounds unless water is present. Therefore, the benefits of water in ethanol under such reacting conditions should lead to savings in operating costs for the energy-intensive removal of water from ethanol and the use of a cheaper ethanol feedstock with high water content.

Keywords: Ethanol; 1,3-butadiene; water; surface response analysis; mixed Hf-Zn catalyst.

1. Introduction

1,3-Butadiene is a valuable conjugated diene which is industrially produced as a co-product of naphtha steam cracking. It is used primarily as a chemical intermediate and as a monomer in the manufacture of synthetic rubbers, most of which are destined to the automobile industry. Despite the financial crisis in 2008, the worldwide automobile industry keeps growing, led by China, which is undergoing a period of explosive development. On the other hand, the onset of the US shale gas has impacted the 1,3-butadiene market as the change in feedstock for steam cracking from naphtha to ethane have resulted in a lower 1,3-butadiene production. Therefore, while the 1,3-butadiene market shrank, the global 1,3-butadiene demand, although shifted to the Asian-Pacific region, continued to grow. In that context, the conversion of bioethanol to 1,3-butadiene arises as an interesting and environmentally friendly alternative in a highly competitive and unstable marketplace [1,2].

The most commonly studied catalyst for the one-step conversion of ethanol to 1,3-butadiene has been MgO/SiO_2 [3-9], originally used in the industrial Lebedev process. The addition of a transition metal, replacement of MgO with one or more transition metal oxides and/or change of type of support (e.g. zeolites), have been thoroughly studied in order to obtain highly selective and stable one-step catalysts [10-30]. In this respect, this work is based on the study by De Baerdemaeker et al. [31] who found that high butadiene yield (up to ~70%, among the highest yields in the literature [11,13,26,32]) could be obtained with the bimetallic system Hf(IV)-Zn(II) when hemimorphite, a crystalline zinc silicate ($Zn_4Si_2O_7(OH)_2 \cdot H_2O$), was used as the source of Zn and then physically mixed with HfO_2/SiO_2. As a promising one-step catalyst (hereafter denoted as mixed Hf-Zn catalyst), practical aspects for its industrial applications, such as the reaction pathway to elucidate the effect of recycling by-products to the reactor and the

catalyst deactivation/regeneration behaviour, were recently studied by our group [33]. In that study, the pathway from ethanol to 1,3-butadiene over the Hf-Zn catalyst was found to concur with the general mechanism proposed in the literature, comprising the following main steps: the dehydrogenation of ethanol to acetaldehyde, the self-aldolization of acetaldehyde to form 3-hydroxybutanal and its further dehydration to crotonaldehyde, the reduction of crotonaldehyde with ethanol via the Meerwein-Ponndorf-Verley (MPV) mechanism to obtain crotyl alcohol, and the dehydration of crotyl alcohol to 1,3-butadiene. The main by-products were ethene and diethyl ether, produced by the dehydration of ethanol; butenes, generated by the hydrogenation of crotyl alcohol to 1-butanol and subsequent dehydration; and heavy products (C_{6+}), resulting from the self- and cross-condensation of alcohols and aldehydes. Besides, it was concluded that the recycle to the reactor of butanal, acetone, and 1-butanol should be avoided since butanal and acetone promote the formation of heavy compounds, related to catalyst deactivation and equipment fouling, while 1-butanol generates butenes which are difficult to separate from 1,3-butadiene.

Other practical aspects that are worth to be studied for the industrial application of a catalyst are the effect of operating conditions and the presence of impurities in the feedstock on catalyst performance. In this regard, the effect of the operating conditions (temperature, space velocity and pressure) on one-step catalysts has not been so widely reported unlike the required acid-base functionalities of catalysts for a selective one-step conversion of ethanol to 1,3-butadiene [6, 34-37]. The operating pressure is usually set at atmospheric pressure as the overall reaction is kinetically fast and not limited by equilibrium at typical operating temperatures (250-450 ºC) [3]. Furthermore, it has been found that increasing the pressure results in higher catalyst deactivation and lower butadiene yield [3,35]. Besides, over a variety of catalysts, the

temperature and weight hourly space velocity (WHSV) deeply affect the ethanol conversion and the yield/selectivity to 1,3-butadiene and by-products. Typically, 1,3-butadiene selectivity is enhanced as the WHSV diminishes because there is more time for the intermediates to be converted to 1,3-butadiene, although a decrease in butadiene selectivity may occur at low WHSV values (i.e., at high ethanol conversions) as side-reactions are more favoured. On the other hand, at constant WHSV, 1,3-butadiene selectivity presents a maximum with temperature due to the fact that the formation of ethene exponentially rises at higher temperatures. Regarding ethanol conversion, it always rises with contact time and temperature [9, 18, 38-41]. So far, the most complete study on the effect of reaction conditions has been reported by Simoni Da Ros et al. [38], who applied statistical experimental design to assess the effect of temperature and space velocity over a K_2O-ZrO_2-ZnO/MgO-SiO_2 catalyst feeding pure ethanol diluted with inert gas. These authors developed a statistical model that correlated the observed product selectivities with the reaction conditions. However, from a process design point of view, the water content in ethanol should also be considered as a factor when modelling the catalyst performance, as explained below.

Water is produced in the reactor (2 moles of water per mole of 1,3-butadiene) so the recovery and recycle of unconverted ethanol involves expensive separation from water, especially beyond the ethanol-water azeotrope (95.5 wt% ethanol). Besides, water can be already present in the ethanol feedstock as ethanol is marketed with different water contents, usually from anhydrous (> 99% v/v ethanol) to industrial grade (~95% v/v ethanol, ~7.5 wt% H_2O) ethanol, and is more expensive as the water content decreases. Evaluating the effect of water content in ethanol on catalyst performance is, thus, necessary to decide to what degree water should be removed from ethanol in order to find a trade-off between reactor performance and the

costs of separation and ethanol feedstock. The Lebedev commercial process fed crude bioethanol (~15 wt% water) to the reactor since the same 1,3-butadiene yield was obtained if rectified ethanol was fed instead (~7.5 wt% water) [42]. Nevertheless, Lebedev and co-workers reported that the effect of water on 1,3-butadiene yield varied with the operating temperature over the MgO/SiO_2 catalyst. At industrial operating temperature (440 ºC), they observed that the presence of water (6-25 wt%) decreased 1,3-butadiene yield while at higher temperature (500 ºC) the opposite was observed [42].

Therefore, the effect of water content in ethanol on catalyst performance should be analyzed with caution as it seems to be temperature dependent. However, in the recent literature, studies on the influence of water content on one-step catalysts are scarce and, furthermore, they do not take into account the temperature effect. Ochoa et al. [7] showed that over MgO/SiO_2 catalyst the presence of water in the ethanol feedstock (equivalent to ca. 70% of the water formed *in situ* during the reaction) decreased the conversion of ethanol and increased the selectivity to ethene, diethyl ether, acetone, and acetaldehyde at the expense of 1,3-butadiene and butene at a reaction temperature of 400 °C. FTIR-pyridine measurements before and after pre-adsorption of water on the catalyst revealed the generation of Brønsted acid sites by interaction of Lewis acid sites with water. This Lewis-to-Brønsted acid sites transformation was postulated to be responsible for the detrimental effect on activity and selectivity of water generated *in situ* during the ethanol-to-1,3-butadiene reaction. Other works have reported the effect of water content on one-step catalysts but using a mixture of ethanol/acetaldehyde as feed, namely, Zhu et al [43] over a Mg/SiO_2 catalyst and Zhang et al. over a $ZnO/ZrO_2/SiO_2$ catalyst [44]. Surprisingly, in these works the selectivity to ethanol dehydration products (ethene and diethyl ether) decreased with water content, just the opposite trend reported by Ochoa et al. [7].

While in the previous studies the effects of the operating conditions and water content in ethanol on the behaviour of one-step catalysts have been investigated separately, we believe that a joint analysis of all the variables is necessary to predict the reactor performance in an industrial process. Therefore, the aim of the present work is to assess the simultaneous effect of operating conditions and water content in ethanol on the performance of the mixed Hf-Zn catalyst, and to build a statistical model of the catalyst performance that allows evaluating how reaction conditions impact variables of interest such as 1,3-butadiene yield and selectivity. Furthermore, the developed model could be used for the conceptual design, optimization, and techno-economic assessment of a one-step ethanol-to-1,3-butadiene process.

2. Materials and methods

2.1. Catalysts preparation and characterization

The catalyst was prepared following the methodology reported in the work by De Baerdemaeker et al. [31] and detailed in our previous work [33]. Briefly, the catalyst was obtained by physically mixing the zinc silicate hemimorphite ($Zn_4Si_2O_7(OH)_2 \cdot H_2O$, abbreviated as HM) and an impregnated Hf/SiO_2 solid (3.5 wt% Hf loading) in a 15:85 weight ratio so as to achieve a nominal composition of 3.0 wt% Hf and 9.3 wt% Zn in the catalyst.

The physicochemical properties of the catalyst determined by a wide set of characterization techniques, including ICP-OES, XRD, STEM-EDX, $^{1}H/^{13}C$ CP-MAS NMR, XPS and IR spectroscopy of adsorbed pyridine and CO, are given and discussed in ref. [33]. Here, we carried out *in situ* IR spectroscopic measurements to study the possible generation of Brønsted acid sites in the mixed Hf-Zn catalyst in the presence of water at reaction conditions. IR spectra in the νOH region were recorded with a Nexus 8700 FTIR spectrometer using a

DTGS detector and acquiring at 4 cm^{-1} resolution. An IR cell allowing *in situ* treatments in controlled atmospheres and temperatures from 25 °C to 500 °C connected to a vacuum system with gas dosing facility was employed in these experiments. Prior to spectra acquisition, the sample was pressed into a self-supported wafer (~10 mg) and activated in vacuum (10^{-5} mbar) at 200 °C for 2 h in order to remove physisorbed water. Next, the sample was exposed to a flow of dry N_2 (10 cm^3/min) and the temperature increased to 380 ºC. At that temperature, the N_2 stream was saturated with 14% and 45% H_2O (by bubbling N_2 through a water-saturator kept at 50 ºC and 70 ºC, respectively). IR spectra were recorded at each step. Additionally, IR experiments of adsorbed pyridine were performed in a dedicated IR cell and the spectra were recorded with a Thermo Nicolet iS10 spectrometer. First, the Hf-Zn catalyst was *in situ* exposed to a flow of dry or wet (45% H_2O) N_2 at 380 ºC. Afterwards, the sample was evacuated at 380 ºC for 10 min, the temperature was decreased to 150 ºC, and 17 mbar of pyridine were introduced in the cell at this temperature. Subsequently, physisorbed pyridine was removed by evacuation at 10^{-3} mbar for 30 min and the IR spectra recorded at 150 ºC. For comparison purposes, the spectra were normalized to sample weight.

2.2. Experimental facility and catalytic tests

Catalytic tests were carried out using the same fixed-bed continuous flow reactor facility and methodology reported in [33]. Prior to reaction, the catalyst was pressed, crushed and sieved to collect the 0.3-0.5 mm fraction, diluted with SiC and deposited in the reactor between two SiC beds. As start-up procedure, the catalyst was preheated at 1 ºC/min to 400 ºC while feeding nitrogen with a mass flow controller. After 10 min at this temperature, the reactor was cooled down to 300 ºC at 1 ºC/min and then liquid reactants were introduced into the reactor using a Bronkhorst mini-coriolis mass flow controller. After 3 hours on stream, the temperature was

raised to the desired operating temperature at 1 ºC/min. The reactor output line was electrically traced and insulated to avoid product condensation before analysis by on-line GC using an Agilent 7890A gas chromatograph.

The simultaneous effect of temperature, weight hourly space velocity (WHSV), and water content in the ethanol feedstock was studied. For all combinations of three temperatures (340, 360, and 380 ºC) and three water contents, four space velocities (1.12, 3.2, 6.1, and either 8 or 9.8 h^{-1}) were assessed consecutively from the largest to the lowest WHSV value. Water contents were chosen as anhydrous grade ethanol (~0 wt%), industrial grade ethanol (~7.5 wt%) and crude ethanol (~15 wt%). Due to equipment limitations, for the tests where water content was 7.5 and 15 wt%, the largest space velocity studied was 8 h^{-1}, instead of 9.8 h^{-1} used in the experiment with anhydrous grade ethanol. To check for catalyst deactivation, the experiment at the highest space velocity (WHSV=9.8 or 8 h^{-1}) was repeated at the end of the run of each temperature-water content combination. Three extra tests were performed at 360 ºC with a water content of 3.75 wt% in order to obtain more information about the water effect at the central temperature. The water content in ethanol feed was obtained by adding the required amount of deionized Milli-Q water to anhydrous ethanol (Panreac 99.8% v/v). All tests were carried out with 0.5 g of catalyst at 1 bar of total pressure with ethanol partial pressure in the feed of 0.21 bar. When water was not added to the feed, the nitrogen flow was adjusted to keep the ethanol partial pressure constant. When water was added to the feed, the necessary amount of nitrogen was replaced by water, therefore keeping constant the ethanol partial pressure and total volumetric flow for a given WHSV. Thus, WHSV is inversely related to contact time. The carbon balance error in the catalytic tests was below 10%, except for the conditions at high

temperature and low WHSV where the elevated presence of heavy compounds raised the error up to 20%.

The ethanol conversion and the selectivity and yield to a given product "i" were calculated as follows:

$$Ethanol\ conversion\ (\%) = X = \frac{Converted\ ethanol}{Fed\ ethanol} \bullet 100$$

$$Selectivity\ to\ i\ (\%) = S_i = \frac{C\ atoms\ to\ product\ i}{C\ atoms\ in\ all\ products} \bullet 100$$

$$Yield\ to\ i\ (\%) = Y_i = \frac{X(\%) \cdot S_i(\%)}{100}$$

In addition, WHSV was defined as the mass flow rate of ethanol (water-free) divided by the mass of catalyst in the reactor.

$$WHSV(h^{-1}) = \frac{mass\ flow\ of\ ethanol\ feed\ \left(\frac{g}{h}\right)}{load\ of catalyst\ (g)}$$

3. Results and discussion

3.1. Effect of temperature and space velocity

The catalytic results at different reaction temperatures, space velocities (WHSV), and water contents in the ethanol feed are gathered in Table S1 of the Supporting Information. First, the effects of reaction temperature and WSHV on catalyst performance are discussed based on the experiments with anhydrous ethanol. Both temperature and WHSV significantly affect the performance of the catalyst. As expected, ethanol conversion (Figure 1) rises with temperature since the overall ethanol-to-1,3-butadiene reaction is not limited by equilibrium in the range of

temperature and pressure of the tests, and linearly decreases with WHSV as the contact time diminishes. This behaviour has also been reported for other one-step catalysts in the previous literature [9, 35, 38-40].

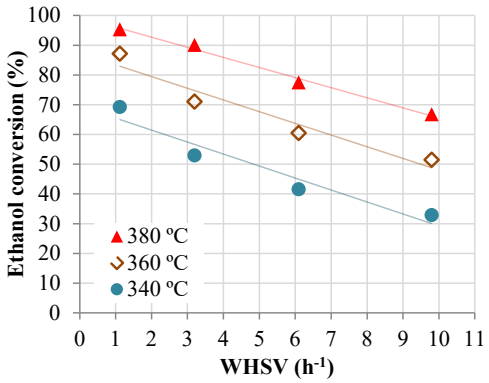

Figure 1. The effect of temperature and WHSV on ethanol conversion over the mixed Hf-Zn catalyst. P= 1 bar, P_{EtOH}= 0.21 bar, feed is anhydrous ethanol.

At 340 and 360 ºC, 1,3-butadiene yield (Figure 2a) increases with ethanol conversion, that is, as WHSV decreases. On the other hand, the acetaldehyde yield (Figure 2b) shows a maximum with ethanol conversion, which confirms that acetaldehyde is an intermediate in the formation of 1,3-butadiene over the mixed Hf-Zn catalyst, as concluded in our previous study [33]. At 380 ºC, however, the yield of 1,3-butadiene barely change with ethanol conversion, at least in the conversion range from 65 to 95% (Figure 2a). The likely reason for this behaviour is that, at this temperature, acetaldehyde is so reactive (steep slope of acetaldehyde curve, Figure 2b) that it is rapidly converted into heavy compounds (C_{6+}) through aldol condensation with itself and heavier aldehydes (Figure 2e). The excessive formation of heavy products results in operational problems, such as faster catalyst deactivation [33,44], and in lower 1,3-butadiene selectivity (Table S1). Furthermore, the formation of ethene and diethyl ether, ethanol dehydration products, and of butenes (1-butene, isobutene, *cis*-2-butene and *trans*-2-butene),

products of butanol dehydration, is also undesired in one-step catalysts in order to avoid low selectivity to 1,3-butadiene. In line with what has been reported elsewhere for other one-step catalysts [9, 18, 35], the yields of ethene and diethyl ether (Figure 2c) and of butenes (Figure 2d) increase with temperature and contact time. However, our results show that these trends stop at high temperature (380 ºC) where the formation of heavy compounds is much more favoured than those products regardless of the WSHV.

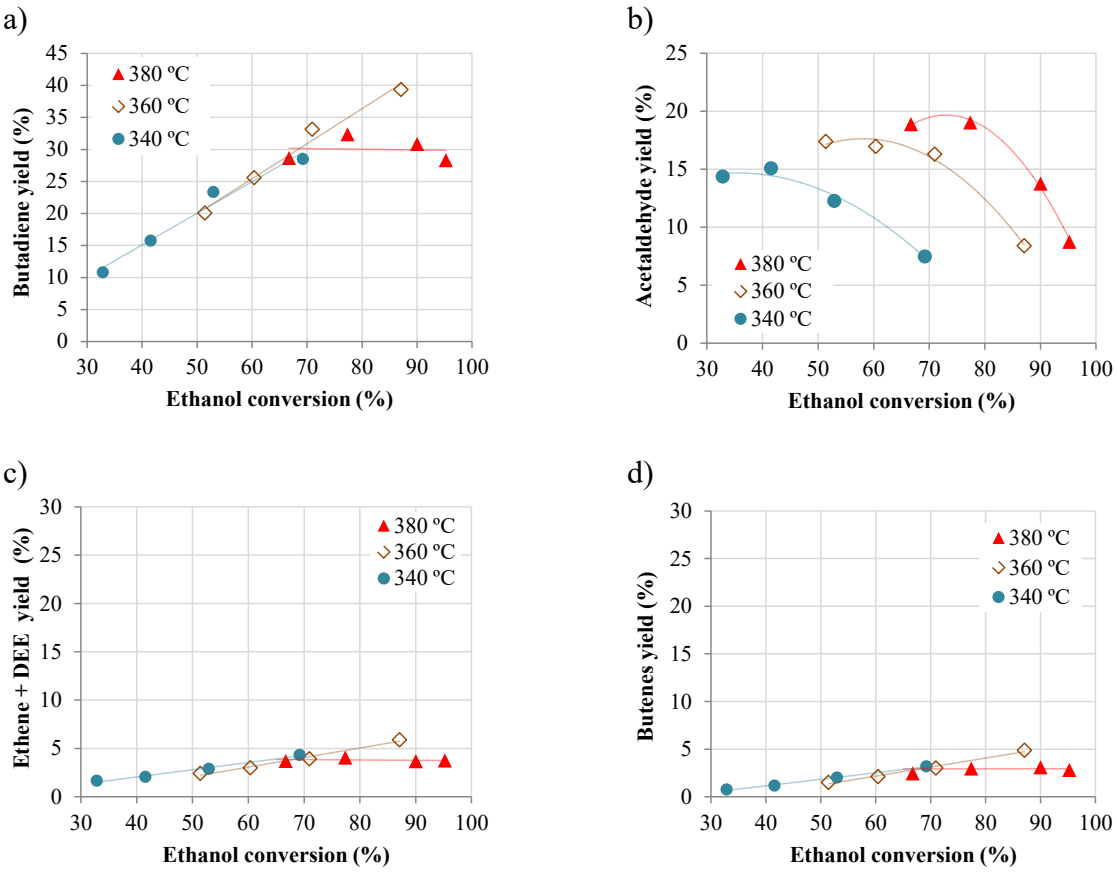

e)

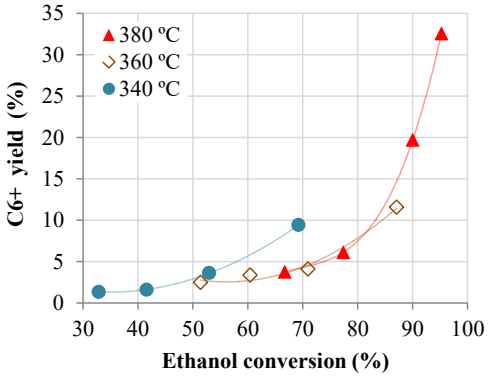

Figure 2. Effect of temperature and WHSV on the yield of a) 1,3-butadiene, b) acetaldehyde, c) ethene plus diethyl ether, d) butenes, and e) heavy products (C_{6+}) over the mixed Hf-Zn catalyst. P= 1 bar, P_{EtOH}= 0.21 bar, feed is anhydrous ethanol.

3.2. Effect of water content in ethanol

The catalytic results obtained in the present study revealed that the presence of water in ethanol severely affects catalyst performance (Table S1, Figure 3). For the sake of simplicity, only the results at 360 and 380 ºC have been plotted in Figure 3, since the tendencies with increasing water content at 340 and 360 ºC are very similar. As seen in Figure 3a, the conversion of ethanol is impaired by the presence of water. The higher the water content, the lower the conversion, but this relationship is not linear. Certainly, at any temperature and space velocity, the decrease in the conversion when increasing the water content from 0 to 7.5 wt% is significantly larger than from 7.5% to 15 wt%. Also, the higher the temperature, the lower the decrease in the ethanol conversion with water content. Subsequently, operating at a high temperature partially counteracts the effect of water on ethanol conversion.

a)

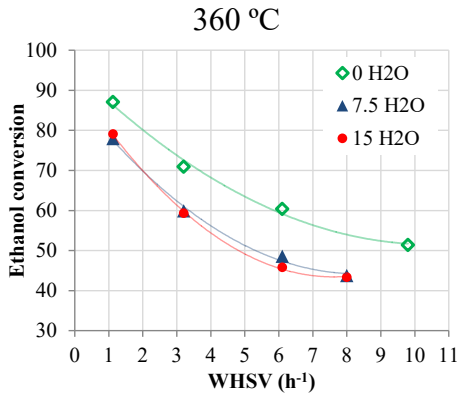
360 ºC
Ethanol conversion
WHSV (h-1)
0 H2O
7.5 H2O
15 H2O

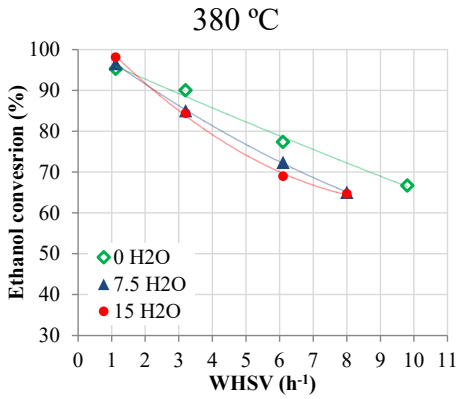
380 ºC
Ethanol conversion (%)
WHSV (h-1)
0 H2O
7.5 H2O
15 H2O

b)

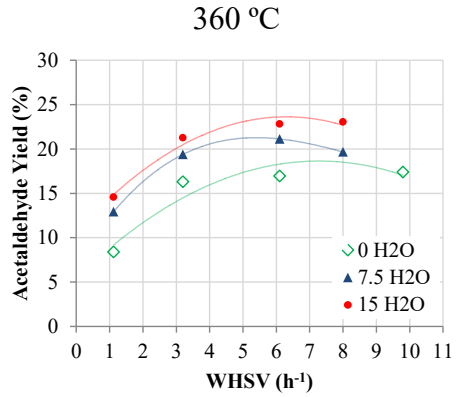
360 ºC
Acetaldehyde Yield (%)
WHSV (h-1)
0 H2O
7.5 H2O
15 H2O

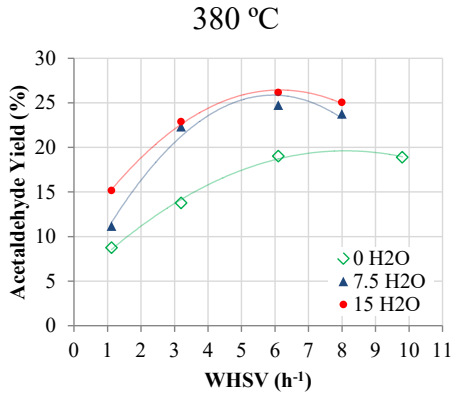
380 ºC
Acetaldehyde Yield (%)
WHSV (h-1)
0 H2O
7.5 H2O
15 H2O

c)

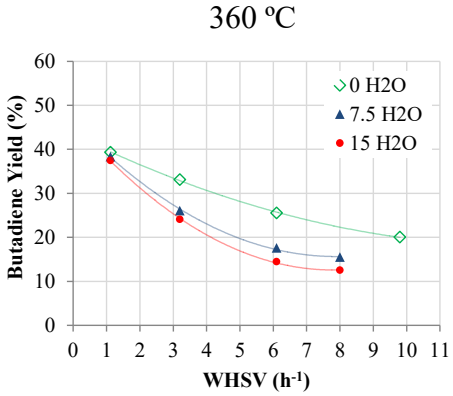
360 ºC
Butadiene Yield (%)
WHSV (h-1)
0 H2O
7.5 H2O
15 H2O

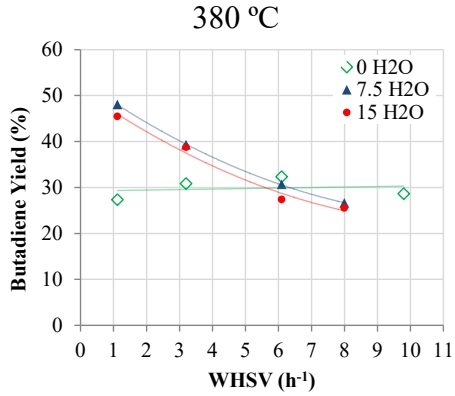
380 ºC
Butadiene Yield (%)
WHSV (h-1)
0 H2O
7.5 H2O
15 H2O

d)

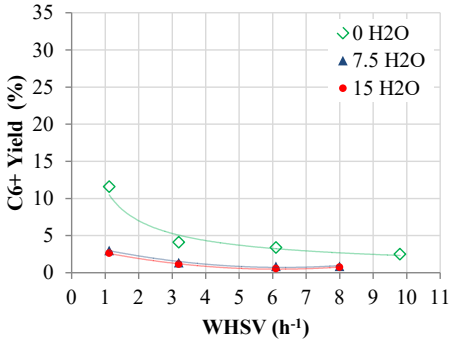
360 ºC
C6+ Yield (%)
WHSV (h-1)
0 H2O
7.5 H2O
15 H2O

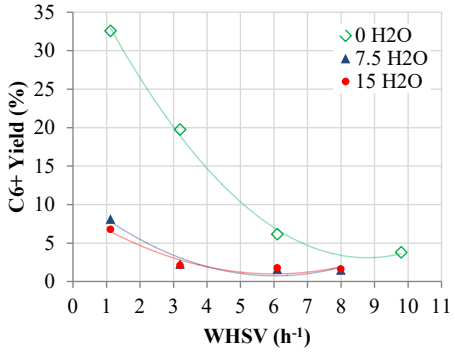
380 ºC
C6+ Yield (%)
WHSV (h-1)
0 H2O
7.5 H2O
15 H2O

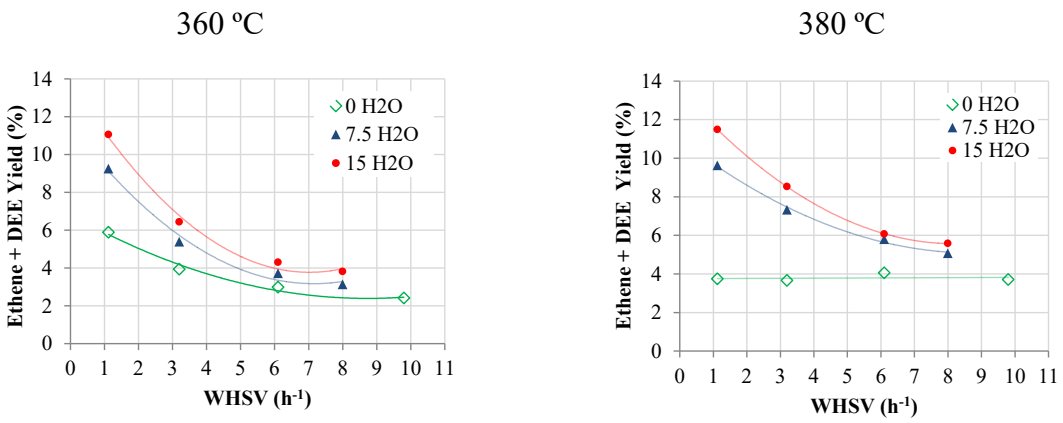

Figure 3. Effect of water content in ethanol feed on a) ethanol conversion, and b)-e) yield to products at 360 °C (left panels) and 380 °C (right panels) as a function of space velocity and water content (wt%) in ethanol.

The decrease in ethanol conversion with water points to the inhibition of ethanol dehydrogenation to acetaldehyde, probably by the competitive adsorption between ethanol and water for Zn-O Lewis acid-base pairs in hemimorphite, which are the active sites for ethanol dehydrogenation in the Hf-Zn catalyst [31]. However, as shown in Figure 3b, the acetaldehyde yield increases with water content. As acetaldehyde is formed by ethanol dehydrogenation and consumed in aldol condensation reactions, the increase in acetaldehyde yield points to a larger inhibition by water of aldol condensation reactions as compared to ethanol dehydrogenation. This is supported by the decrease in the yield to 1,3-butadiene and heavy products, as observed in Figure 3c (left) and 3d, respectively. Inhibition of aldol condensations by water is expected to occur by blocking of Lewis acid sites active for these reactions [45] which, in the case of our Hf-Zn catalyst, have been associated to Hf^{4+} species [31]. Differently, at high temperature (380 ºC) and low space velocity, where the formation of heavy compounds (C_{6+}) is significant for an anhydrous ethanol feedstock (Figure 3d, right), the presence of water results in an increase of the

yield to 1,3-butadiene (Figure 3c, right). This indicates that, at 380 ºC, formation of heavy products is inhibited to a larger degree than that of 1,3-butadiene. This could be explained considering that a reduction in the concentration of available active Hf^{4+} sites due to water adsorption will decrease the probability of occurrence of consecutive aldol condensation reactions through which heavy products are formed [30].

On the other hand, the effect of water content in ethanol on formation of butenes is, at any temperature, similar to that of 1,3-butadiene (Figure S3), an expectable result considering that self-condensation of acetaldehyde is also an intermediate reaction step in the formation of butenes [33].

Other observation is that, at any temperature, the presence of water increases the formation of direct ethanol dehydration products, ethene and diethyl ether (Figure 3e). This behaviour suggests an increase in the Brønsted acidity of the catalyst, probably by transformation of some of the Lewis acid sites into Brønsted acid sites by water chemisorption. This transformation could also contribute, besides the blocking of Lewis acid sites, to the lower activity of the catalyst in the presence of water (Figure 3a). The generation of additional Brønsted acid sites in the mixed Hf-Zn catalyst induced by water is addressed in the next section 3.3 based on *in situ* IR spectroscopic experiments.

Finally, as shown in Figure S4 (Supporting Information), the deactivation rate of the mixed Hf-Zn catalyst (at 360 ºC) decreases by a factor of ca. 8.5 when feeding hydrous (7.5 wt% water) versus anhydrous ethanol. The remarkably higher stability of the catalyst in presence of water might be ascribed, at least in part, to the inhibited formation of heavy products which are coke precursors ultimately promoting catalyst deactivation [30]. Moreover, as we showed in our previous work [33], the coke deposited on the Hf-Zn catalyst in experiments feeding anhydrous

ethanol comprised mainly bulky oxygenated aromatic compounds likely produced through consecutive condensation and dehydrogenation reactions. Therefore, the limited dehydrogenation ability of the catalyst due to blocking of Lewis acid sites, predominantly those associated to Zn^{2+} cations displaying a stronger acidity than Hf^{4+} [33], and to their (partial) transformation into Brønsted acid sites, as will be discussed next, is anticipated to contribute to the much lower deactivation rate observed in presence of water.

3.3. Water-induced formation of Brønsted acid sites followed by IR spectroscopy

The IR spectra in the νOH region of the mixed Hf-Zn catalyst and its components in the physical mixture hemimorphite (HM) and Hf/SiO_2 recorded after *in situ* activation at 200 °C are shown in Figure S1 of Supporting Information. The spectrum of the mixed Hf-Zn catalyst shows the presence of different –OH groups characterized by IR bands peaking at 3737, 3666, 3602, and 3545 cm^{-1} (spectrum c). The intense sharp band at 3737 cm^{-1} corresponds to Si-OH groups in the amorphous SiO_2 carrier and, as expected, is also present in the spectrum of the Hf/SiO_2 component (spectrum b). The broad band at about 3666 cm^{-1}, which is also observed in Hf/SiO_2 (spectrum b), is assigned to –OH groups associated with Hf^{4+} ions, while the lower frequency bands at 3602 and 3545 cm^{-1} are clearly related to –OH groups in the zinc silicate hemimorphite (spectrum a).

After activation in vacuum at 200 °C, the mixed Hf-Zn catalyst sample in the IR cell was heated at 380 °C and the spectrum in the νOH region was recorded at this temperature under dry and wet (14 and 45 wt% water) N_2 flow. The corresponding IR spectra are depicted in Figure 4. We selected 380 °C for the IR experiments as this was the highest temperature employed in the catalytic tests and for which the water effects were more pronounced, as discussed above. It can

be seen in Figure 4 that heating the mixed Hf-Zn catalyst at 380 ºC under flowing dry N_2 (spectrum b) produces a decrease in the intensity of the bands at 3666, 3602, and 3545 cm^{-1} of Hf- and Zn-related –OH groups with respect to the sample activated in vacuum at 200 ºC (spectrum a) due to dehydroxylation. Interestingly, in the presence of 45% water (spectrum c) at the same temperature, a new sharp band emerges at 3588 cm^{-1} that unambiguously indicates the generation of additional –OH groups. Similar results were obtained at a water content in the N_2 stream of 14 wt% (not shown). Although an unequivocal assignment of the new OH band to either Hf or Zn species is not straightforward from our results, it seems reasonable to assume that they are probably related to Zn^{2+} species in hemimorphite since, according to our previous study [33], they exhibit a stronger Lewis acid character than Hf^{4+} and should be, thus, more prone to react with water. The fact that the newly developed IR band remains even after evacuation of the sample at 380 °C in vacuum (spectrum d) signs for its high stability. This is in line with previous studies reporting a high thermal stability (up to 350 ºC) of surface hydroxyls generated by chemisorption of water over ZnO [46]. Therefore, we expect the newly formed surface hydroxyls to be present in the catalyst during the catalytic experiments with co-fed water at the studied reaction conditions.

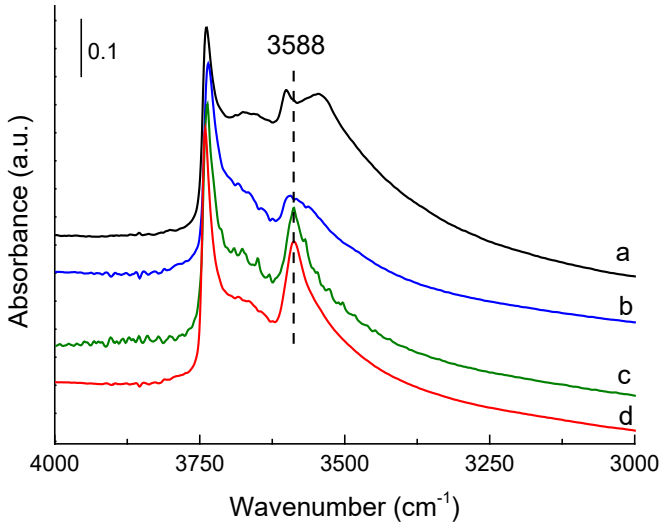

Figure 4. IR spectra of the mixed Hf-Zn catalyst in the νOH region after activation in vacuum at 200 °C (a), under dry N_2 flow at 380 °C (b), under wet N_2 flow (45% water) at 380 ºC (c), and after a final evacuation in vacuum at 380 ºC (d).

In order to ascertain whether the –OH groups at 3588 cm^{-1} generated in situ in the presence of water entails the formation of new Brønsted acid sites, we performed IR experiments of adsorbed pyridine after in situ submitting the Hf-Zn catalyst to a flow of dry or wet (45% water) nitrogen at the reaction temperature of 380 °C. The IR spectra in the pyridine vibration region at a desorption temperature of 150 ºC are shown in Figure 5. As observed, the Hf-Zn catalyst exhibits mainly Lewis-type acidity, characterized by the IR band at ca. 1445 cm^{-1}, in agreement with previous studies [31,33]. Nonetheless, a very low intense band at ca. 1545 cm^{-1} can be perceived in the spectrum of the sample treated in dry N_2 (spectrum a), signing for the presence of a minor amount of Brønsted acid sites (BAS). Indeed, the presence of BAS in the calcined Hf-Zn catalyst was unambiguously identified in our previous work by using low-temperature IR spectroscopy of adsorbed CO [33]. Furthermore, the spectrum of pyridine

adsorbed on the Hf-Zn sample previously submitted to wet (45% water) N_2 flow clearly evidences an increase in the intensity of the band at ca. 1545 cm^{-1} associated to BAS (spectrum b and zoomed view in the inset of Figure 5). This result indicates that the new –OH groups at 3588 cm^{-1} developed in the water-treated sample (Figure 4) exhibit Brønsted acidity of medium strength. Unfortunately, quantification of the amount of acid sites by IR-pyridine is not straightforward due to the lack of precise molar extinction coefficients for this kind of materials.

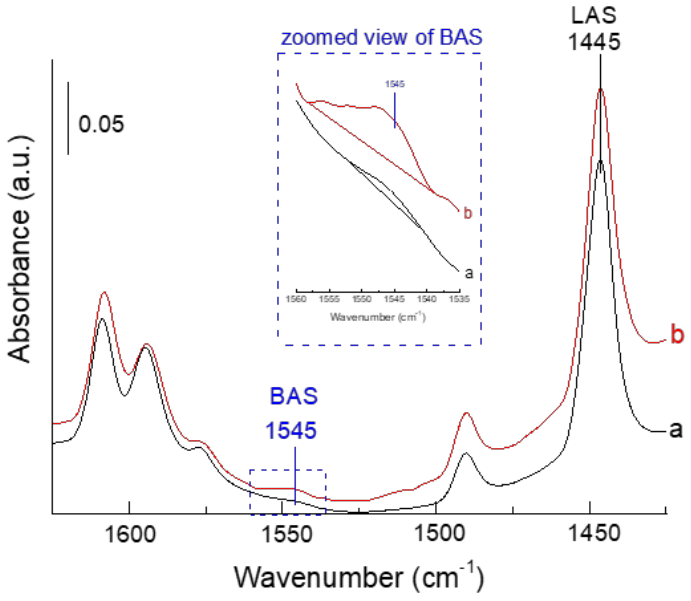

Figure 5. IR spectra in the pyridine vibration region at a pyridine desorption temperature of 150 ºC for the Hf-Zn catalyst after in situ treatment under flowing dry (spectrum a) and wet (45% water) N_2 at 380 ºC.

In conclusion, the above *in situ* IR measurements demonstrate the generation of new Brønsted acid sites in the presence of water at the employed reaction conditions, probably by reaction of Zn^{2+} Lewis acid sites with water. This would explain the changes in catalyst behavior

observed when feeding ethanol-water mixtures, particularly at the highest reaction temperature of 380 ºC (section 3.2).

3.4. Response surface analysis

The effect of reaction conditions on ethanol conversion (X) and product selectivity (S_i) and yield (Y_i) over the mixed Hf-Zn catalyst was studied using a response surface analysis with the statistical software StatGraphics®. These response variables ($\hat{y}$) were regressed with a second-order equation in the form of Eq. 1 where T is the temperature in ºC, W is the content of water in the ethanol feed in wt%, and WHSV is the space velocity in h^{-1}. The experimental data were divided into two data sets, one for the fitting and another for the validation of the model, as explained below. The parameters were fitted by linear least squares, rejecting the terms not statistically significant with a confidence level of 95% based on the p-values. The residuals analysis (not shown) confirmed the normality, homoscedasticity and linearity hypothesis.

$$\hat{y} = a_0 + a_1 \cdot T + a_2 \cdot W + a_3 \cdot WHSV + a_4 \cdot T^2 + a_5 \cdot T \cdot W + a_6 \cdot T \cdot WHSV + a_7 \cdot W^2 + a_8 \cdot W \cdot WHSV + a_9 \cdot WHSV^2 \quad \text{Eq. 1}$$

Table 1 shows the fitted parameters and the coefficients of determination (R^2) of the regressions, which are relatively high (90-98%). The selectivity to acetaldehyde, 1,3-butadiene, butenes, acetaldehyde, and heavy products as well as the yield of 1,3-butadiene were better fitted when their natural logarithm was chosen as response variable. The good agreement between the experimental data and the values predicted by the model is clearly inferred from the parity plots shown in Figure S2 of Supporting Information.

Table 1. Estimated parameters of Equation 1 for response variables.

Parameters	X	Ln(Y_{BD})	Ln(S_{BD})	Ln(S_{AC})	S_{ET}	S_{DEE}	Ln(S_{C4})	Ln(S_{C6+})
a_o	-207.108	-30.456	-18.715	6.036	-190.691	16.224	-23.786	104.250
a_1	0.838	0.194	0.136	-0.012	1.105	-0.042	0.151	-0.580
a_2	-7.188	-0.475	-0.268	0.084	0.674	0.644	-0.326	-0.226
a_3	-8.619	-1.300	-0.793	0.412	-2.751	-1.286	-1.030	-0.315
a_4	-	-0.0003	-0.0002	-	-0.002	-	-0.0002	0.0008
a_5	0.016	0.0014	0.0008	-	-	-0.001	0.0009	-
a_6	-	0.0034	0.0022	-	0.005	0.004	0.0024	-
a_7	0.051	-	-0.0010	-0.0024	-0.019	-0.007		0.009
a_8	-	-0.007	-0.0053	-0.0032	-0.025	-0.005	-0.0061	-
a_9	0.421	-	-	-0.0254	0.068	-	0.0093	0.019
R^2	98.5	96.8	89.6	97.8	92.4	95.2	94.6	90.7

Note: BD= butadiene; AC=Acetaldehyde; ET=ethene; DEE=diethyl ether; C4= butenes; C6+= heavy compounds

Two tests at different temperature, water content, and space velocity were set aside to validate the statistic model. As shown in Table 2, the validation data set is reasonably well predicted. The largest absolute prediction error is associated to acetaldehyde selectivity, but its relative error is small (~6%). Therefore, a good generalization capability of the model is expected within the employed range of reaction conditions (section 2.2).

Table 2. Prediction of response variables for the validation data set.

Op. Cond.		Value	X (%)	Y_{BD}(%)	S_{BD}(%)	S_{AC}(%)	S_{ET}(%)	S_{DEE} (%)	S_{C4}(%)	S_{C6+} (%)
T (ºC)	340	Measured	41.56	15.76	37.93	36.25	3.33	1.64	2.81	3.85
W (%)	0	Estimated	40.76	15.82	36.36	33.98	2.53	1.68	2.62	4.81
WHSV (h^{-1})	6.1	Abs. Error	0.80	0.06	1.57	2.27	0.80	0.04	0.19	0.96
T (ºC)	360	Measured	43.40	12.50	28.80	53.10	6.40	2.40	1.60	1.70
W (%)	15	Estimated	43.18	10.70	27.81	49.83	6.58	2.22	1.66	1.03
WHSV (h^{-1})	8	Abs. Error	0.22	1.80	0.99	3.27	0.18	0.18	0.06	0.67

Note: BD= butadiene; AC=Acetaldehyde; ET=ethene; DEE=diethyl ether; C4= butenes; C6+= heavy compounds

The response surface analysis allows distinguishing how reaction conditions impact variables of interest such as 1,3-butadiene yield and selectivity (Figure 6). For instance, when the

water content in ethanol is 7.5%, the 1,3-butadiene yield is maximized at low space velocity and high operating temperature (Figure 6b, left), which involves high ethanol conversion (Figure 6a, left) and also high butadiene selectivity (Figure 6c, left). Other conclusions are not so straightforward. At 360 ºC and relatively low space velocities (< 5 h^{-1}), the 1,3-butadiene yield is almost insensitive to the water content in ethanol (Figure 6b, right) since contour plots are flat. This is a consequence of the fact that, at 360 ºC and fixed space velocity, as water content increases ethanol conversion decreases but 1,3-butadiene selectivity increases, and both effects counterbalance. Certainly, this is in agreement with the effect of water content in ethanol reported by Lebedev and co-workers operating at a high temperature with the Lebedev catalysts [42]. We see that the statistical model allows taking into account the interaction between process variables that are not intuitive.

a) Ethanol conversion

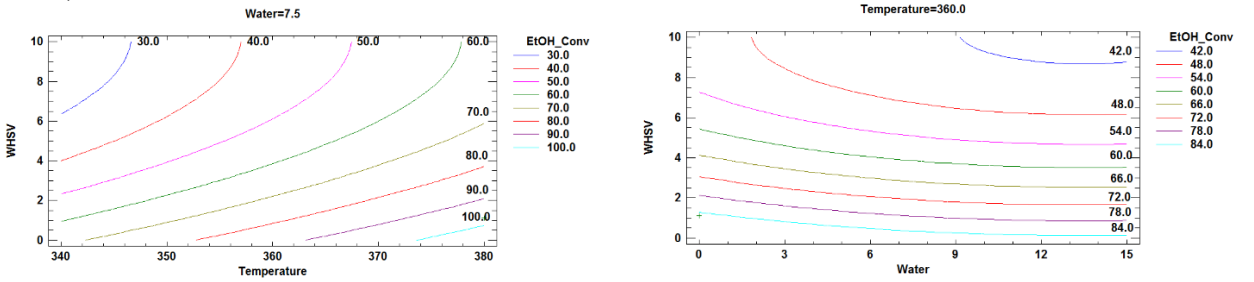

b) 1,3-butadiene yield

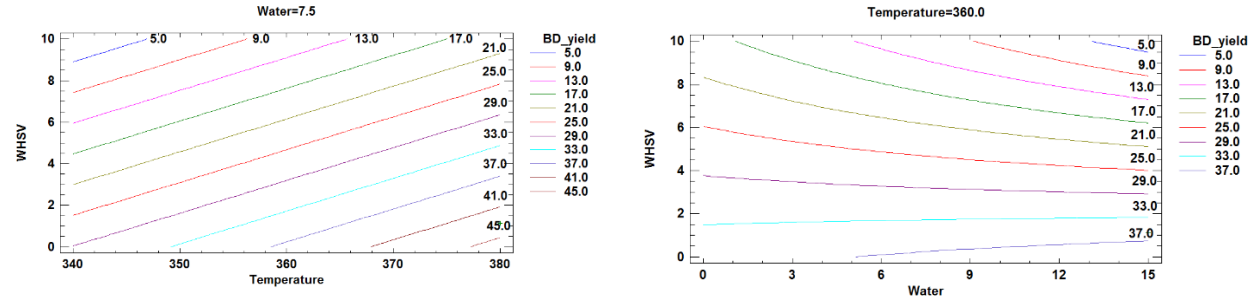

c) 1,3-butadiene selectivity

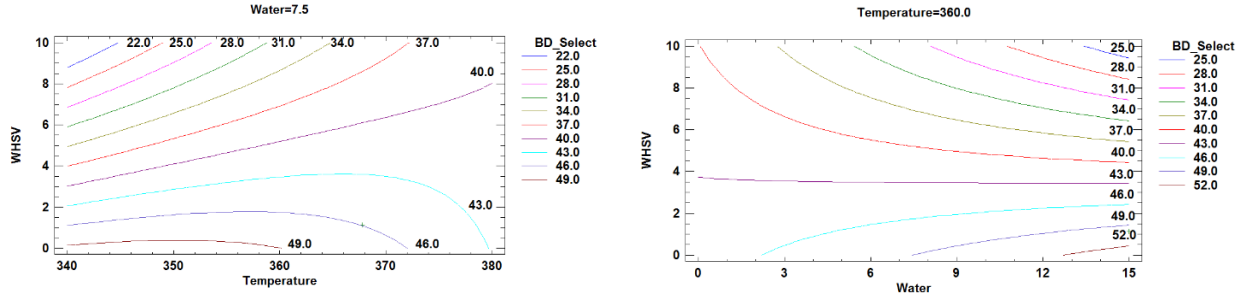

d) C_{6+} selectivity

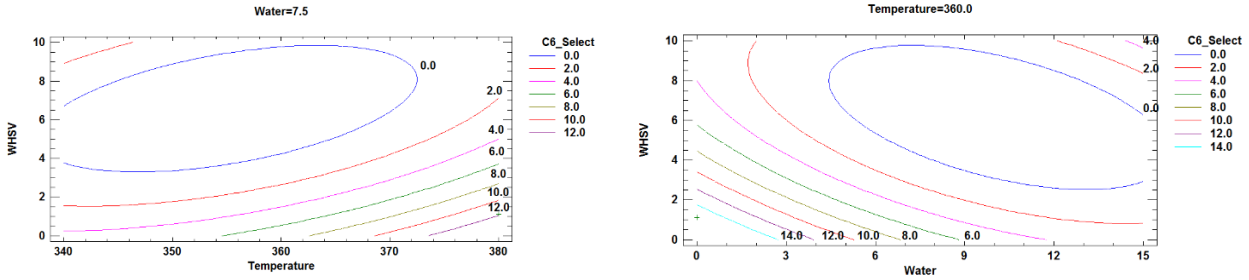

Figure 6. Parametric curves of the response surface analysis model for a) ethanol conversion, b) 1,3-butadiene yield, c) 1,3-butadiene selectivity, d) C_{6+} selectivity. Temperatures in ºC, WHSV in h^{-1}, and water content in wt%.

As an application of the statistical model for process design, it was used to study which combination of operating variables maximized 1,3-butadiene selectivity or yield. As can be seen in Table 3, the highest 1,3-butadiene yield achievable within the bounds of the process variables studied is 50.62%, which involves operating at the highest temperature and lowest spatial velocity with the highest concentration of water in the feedstock (T= 380 ºC, WHSV= 1.12 h^{-1} and 15 wt% water). This operating point seems to be the finest since the presence of water causes a drastic decrease in the formation of heavy compounds. The operating conditions for maximum 1,3-butadiene selectivity (T= 368 ºC, WHSV= 1.12 h^{-1} and 15 wt% water) are close to that of the maximum 1,3-butadiene yield. In fact, similar 1,3-butadiene selectivity is achieved in both scenarios but, in this case, the 1,3-butadiene yield is lower. It should be noted that the maximum

yield operating point might not be the best operating condition in economic terms, as many trade-offs in the design of the process are involved such as feedstock, reactor and separation costs. Thus, selection of the best operating point of the reactor should be done within the design of the whole process with the aid of the statistical model.

Table 3. Operating conditions for maximum yield or selectivity to 1,3-butadiene.

	Max. yield	**Max. selectivity**
Operating conditions		
Temperature (ºC)	380	368
Water in ethanol (%wt)	15	15
WHSV (h^{-1})	1.12	1.12
Ethanol conversion and main product selectivities (%)		
X	97.65	84.69
Y_{BD}	**50.62**	43.63
S_{BD}	50.04	**51.44**
S_{AC}	15.89	18.25
S_{ET}	10.26	10.82
S_{DEE}	1.54	2.21
S_{C4}	5.43	5.35
S_{C6+}	5.41	3.36
S_{Others}	11.4	8.57

Note: BD= butadiene; AC=Acetaldehyde; ET=ethene; DEE=diethyl ether; C4= butenes; C6+= heavy compounds. "Others" comprises a mixture of minor sub-products such as acetone, ethyl acetate, butanal, butanol, 2-ethyl-hexenal, CO, CO_2 and CH_4.

4. Conclusions

The combined effect of temperature, space velocity and water content in the ethanol feed on the performance of a one-step mixed Hf-Zn catalyst for the conversion of ethanol into 1,3-butadiene has been studied for the first time. The consideration of water content as a process variable in the catalyst performance allows to assess the option of using a cheaper ethanol feedstock instead of anhydrous grade, and to decide to what degree water should be removed from unconverted ethanol in the conceptual design of the process in order to find a trade-off between reactor performance and separation costs. The results of catalyst performance indicate that the presence of water in the ethanol feed enhances the selectivity to dehydration products,

i.e., ethene and diethyl ether from ethanol and decreases ethanol conversion. The increased dehydration activity can be accounted for by the generation of new Brønsted acid sites of medium strength in the mixed Hf-Zn catalyst, as assessed by *in situ* IR spectroscopy, probably by reaction of Zn^{2+}-related Lewis acid sites (active for ethanol dehydrogenation) with water at reaction conditions. Besides this, blocking of Zn^{2+} sites by water represents a loss of dehydrogenation sites resulting in the observed decrease in ethanol conversion. Moreover, water seems to hinder aldol condensation reactions to a greater degree than dehydrogenation due to blocking of Hf^{4+}-related Lewis acid sites. This effect can be beneficial at a high operating temperature, where acetaldehyde is so reactive that it is rapidly converted into heavy compounds unless water is present, allowing higher 1,3-butadiene yield with lower heavy compounds formation. Finally, the presence of water significantly decreases the rate of catalyst deactivation, which can be ascribed to the inhibition of successive condensation and dehydrogenation reactions involved in coke formation. The results of this work are expected to be valid for other bimetallic silica-supported catalysts developed for the one-step conversion of ethanol to 1,3-butadiene.

Acknowledgements

This work has been carried out in the framework of the project "Biobutadiene production from bioethanol" (CTQ2015-71427-R) funded by the Spanish Ministry of Economy, Industry and Competitiveness (MINECO) through the European Regional Development Fund (ERDF). The authors would like to thank Francisco Javier Rueda Lillo for his valuable help in conducting the experimental tests.

References

[1] I. Grand View Research, Global 1,3 Butadiene (BD) Market By Application (SBR, Butadiene Rubber, SB Latex, ABS, HMDA, NBR) Expected To Reach USD 33.01 Billion By 2020: Grand View Research, Inc, Gd. View Res. (2015) 2–5.

[2] REN21, Renewables 2017: global status report, 2017. doi:10.1016/j.rser.2016.09.082.

[3] E. V. Makshina, M. Dusselier, W. Janssens, J. Degrève, P.A. Jacobs, B.F. Sels, Review of old chemistry and new catalytic advances in the on-purpose synthesis of butadiene, Chem. Soc. Rev. 43 (2014) 7917–7953. doi:10.1039/C4CS00105B.

[4] C. Angelici, B.M. Weckhuysen, P.C.A. Bruijnincx, Chemocatalytic conversion of ethanol into butadiene and other bulk chemicals, ChemSusChem. 6 (2013) 1595–1614. doi:10.1002/cssc.201300214.

[5] C. Angelici, M.E.Z. Velthoen, B.M. Weckhuysen, P.C.A. Bruijnincx, Effect of Preparation Method and CuO Promotion in the Conversion of Ethanol into 1,3-Butadiene over SiO2–MgO Catalysts, ChemSusChem. 7 (2014) 2505–2515. doi:10.1002/cssc.201402361.

[6] C. Angelici, M.E.Z. Velthoen, B.M. Weckhuysen, P.C.A. Bruijnincx, Influence of acid-base properties on the Lebedev ethanol-to-butadiene process catalyzed by SiO_2/MgO materials, Catal. Sci. Technol. 5 (2015) 2869–2879. doi:10.1039/c5cy00200a.

[7] J.V. Ochoa, C. Bandinelli, O. Vozniuk, A. Chieregato, A. Malmusi, C. Recchi, F. Cavani, An analysis of the chemical, physical and reactivity features of MgO–SiO_2 catalysts for butadiene synthesis with the Lebedev process, Green Chem. 18 (2016) 1653–1663. doi:10.1039/C5GC02194D.

[8] S.H. Chung, C. Angelici, S.O.M. Hinterding, M. Weingarth, M. Baldus, K. Houben, B.M. Weckhuysen, P.C.A. Bruijnincx, Role of magnesium silicates in wet-kneaded silica-

magnesia catalysts for the Lebedev ethanol-to-butadiene process, ACS Catal. 6 (2016) 4034–4045. doi:10.1021/acscatal.5b02972.

[9] X. Huang, Y. Men, J. Wang, W. An, Y. Wang, Highly active and selective binary MgO–SiO_2 catalysts for the production of 1,3-butadiene from ethanol, Catal. Sci. Technol. 7 (2017) 168–180. doi:10.1039/C6CY02091G.

[10] V.L. Sushkevich, D. Palagin, I.I. Ivanova, With Open Arms: Open Sites of ZrBEA Zeolite Facilitate Selective Synthesis of Butadiene from Ethanol, ACS Catal. 5 (2015) 4833–4836. doi:10.1021/acscatal.5b01024.

[11] T. Yan, W. Dai, G. Wu, S. Lang, M. Hunger, N. Guan, L. Li, Mechanistic Insights into One-Step Catalytic Conversion of Ethanol to Butadiene over Bifunctional Zn-Y/Beta Zeolite, ACS Catal. 8 (2018) 2760–2773. doi:10.1021/acscatal.8b00014.

[12] P. Müller, S.-C. Wang, S.P. Burt, I. Hermans, Influence of Metal Doping on the Lewis Acid Catalyzed Production of Butadiene from Ethanol Studied by using Modulated Operando Diffuse Reflectance Infrared Fourier Transform Spectroscopy and Mass Spectrometry, ChemCatChem. 9 (2017) 3572–3582. doi:10.1002/cctc.201700698.

[13] P.I. Kyriienko, O. V. Larina, S.O. Soloviev, S.M. Orlyk, C. Calers, S. Dzwigaj, Ethanol Conversion into 1,3-Butadiene by the Lebedev Method over MTaSiBEA Zeolites (M = Ag, Cu, Zn), ACS Sustain. Chem. Eng. 5 (2017) 2075–2083. doi:10.1021/acssuschemeng.6b01728.

[14] V.L. Sushkevich, I.I. Ivanova, Ag-promoted ZrBEA zeolites obtained by post-synthetic modification for conversion of ethanol to butadiene, ChemSusChem. 9 (2016) 2216–2225. doi:10.1002/cssc.201600572.

[15] C. Angelici, F. Meirer, A.M.J. Van Der Eerden, H.L. Schaink, A. Goryachev, J.P.

Hofmann, E.J.M. Hensen, B.M. Weckhuysen, P.C.A. Bruijnincx, Ex Situ and Operando Studies on the Role of Copper in Cu-Promoted SiO_2-MgO Catalysts for the Lebedev Ethanol-to-Butadiene Process, ACS Catal. 5 (2015) 6005–6015. doi:10.1021/acscatal.5b00755.

[16] S. Shylesh, A.A. Gokhale, C.D. Scown, D. Kim, C.R. Ho, A.T. Bell, From Sugars to Wheels: The Conversion of Ethanol to 1,3-Butadiene over Metal-Promoted Magnesia-Silicate Catalysts, ChemSusChem. 9 (2016) 1462–1472. doi:10.1002/cssc.201600195.

[17] V.L. Sushkevich, I.I. Ivanova, Mechanistic study of ethanol conversion into butadiene over silver promoted zirconia catalysts, Appl. Catal. B Environ. 215 (2017) 36–49. doi:10.1016/j.apcatb.2017.05.060.

[18] S. Da Ros, M.D. Jones, D. Mattia, J.C. Pinto, M. Schwaab, F.B. Noronha, S.A. Kondrat, T.C. Clarke, S.H. Taylor, Ethanol to 1,3-Butadiene Conversion by using ZrZn-Containing MgO/SiO2Systems Prepared by Co-precipitation and Effect of Catalyst Acidity Modification, ChemCatChem. 8 (2016) 2376–2386. doi:10.1002/cctc.201600331.

[19] V.L. Sushkevich, I.I. Ivanova, V. V. Ordomsky, E. Taarning, Design of a Metal-Promoted Oxide Catalyst for the Selective Synthesis of Butadiene from Ethanol, ChemSusChem. 7 (2014) 2527–2536. doi:10.1002/cssc.201402346.

[20] M.D. Jones, C.G. Keir, C. Di Iulio, R.A.M. Robertson, C. V. Williams, D.C. Apperley, Investigations into the conversion of ethanol into 1,3-butadiene, Catal. Sci. Technol. 1 (2011) 267. doi:10.1039/c0cy00081g.

[21] B.B. Corson, H.E. Jones, C.E. Welling, J.A. Hinckley, E.E. Stahly, Butadiene from Ethyl Alcohol. Catalysis in the One-and Two-Stop Processes., Ind. Eng. Chem. 42 (1950) 359–373. doi:10.1021/ie50482a039.

[22] Y. Kitayama, M. Satoh, T. Kodama, Preparation of large surface area nickel magnesium silicate and its catalytic activity for conversion of ethanol into buta-1,3-diene, Catal. Letters. 36 (1996) 95–97. doi:10.1007/BF00807211.

[23] M. Lewandowski, G.S. Babu, M. Vezzoli, M.D. Jones, R.E. Owen, D. Mattia, P. Plucinski, E. Mikolajska, A. Ochenduszko, D.C. Apperley, Investigations into the conversion of ethanol to 1,3-butadiene using $MgO:SiO_2$ supported catalysts, Catal. Commun. 49 (2014) 25–28. doi:10.1016/j.catcom.2014.02.003.

[24] O. V. Larina, P.I. Kyriienko, S.O. Soloviev, Ethanol Conversion to 1,3-Butadiene on $ZnO/MgO-SiO_2$ Catalysts: Effect of ZnO Content and $MgO:SiO_2$ Ratio, Catal. Letters. 145 (2015) 1162–1168. doi:10.1007/s10562-015-1509-4.

[25] O. V. Larina, P.I. Kyriienko, V. V. Trachevskii, N. V. Vlasenko, S.O. Soloviev, Effect of Mechanochemical Treatment on Acidic and Catalytic Properties of $MgO-SiO_2$ Composition in the Conversion of Ethanol To 1,3-Butadiene, Theor. Exp. Chem. 51 (2016) 387–393. doi:10.1007/s11237-016-9440-3.

[26] V.L. Dagle, M.D. Flake, T.L. Lemmon, J.S. Lopez, L. Kovarik, R.A. Dagle, Effect of the SiO2support on the catalytic performance of $Ag/ZrO_2/SiO_2$ catalysts for the single-bed production of butadiene from ethanol, Appl. Catal. B Environ. 236 (2018) 576–587. doi:10.1016/j.apcatb.2018.05.055.

[27] R.A.L. Baylon, J. Sun, Y. Wang, Conversion of ethanol to 1,3-butadiene over Na doped ZnxZryOzmixed metal oxides, Catal. Today. 259 (2016) 446–452. doi:10.1016/j.cattod.2015.04.010.

[28] Y. Hayashi, S. Akiyama, A. Miyaji, Y. Sekiguchi, Y. Sakamoto, A. Shiga, T. Koyama, K. Motokura, T. Baba, Experimental and computational studies of the roles of MgO and Zn

in talc for the selective formation of 1,3-butadiene in the conversion of ethanol, Phys. Chem. Chem. Phys. 18 (2016) 25191–25209. doi:10.1039/C6CP04171J.

[29] W. Dai, S. Zhang, Z. Yu, T. Yan, G. Wu, N. Guan, L. Li, Zeolite Structural Confinement Effects Enhance One-Pot Catalytic Conversion of Ethanol to Butadiene, ACS Catal. 7 (2017) 3703–3706. doi:10.1021/acscatal.7b00433.

[30] L. Yang, M. Hunger, W. Dai, L. Li, T. Yan, G. Wu, C. Wang, N. Guan, On the deactivation mechanism of zeolite catalyst in ethanol to butadiene conversion, J. Catal. 367 (2018) 7–15. doi:10.1016/j.jcat.2018.08.019.

[31] T. De Baerdemaeker, M. Feyen, U. Müller, B. Yilmaz, F.S. Xiao, W. Zhang, T. Yokoi, X. Bao, H. Gies, D.E. De Vos, Bimetallic Zn and Hf on silica catalysts for the conversion of ethanol to 1,3-butadiene, ACS Catal. 5 (2015) 3393–3397. doi:10.1021/acscatal.5b00376.

[32] G. Pomalaza, G. Vofo, M. Capron, F. Dumeignil, ZnTa-TUD-1 as an easily prepared, highly efficient catalyst for the selective conversion of ethanol to 1,3-butadiene, Green Chem. 20 (2018) 3203–3209. doi:10.1039/c8gc01211c.

[33] G.M. Cabello González, R. Murciano, A.L. Villanueva Perales, A. Martínez, F. Vidal-Barrero, M. Campoy, Ethanol conversion into 1,3-butadiene over a mixed Hf-Zn catalyst: A study of the reaction pathway and catalyst deactivation, Appl. Catal. A Gen. 570 (2019) 96–106. doi:10.1016/J.APCATA.2018.11.010.

[34] A. Klein, K. Keisers, R. Palkovits, Formation of 1,3-butadiene from ethanol in a two-step process using modified zeolite-β catalysts, Appl. Catal. A Gen. 514 (2016) 192–202. doi:10.1016/j.apcata.2016.01.026.

[35] W. Janssens, E. V. Makshina, P. Vanelderen, F. De Clippel, K. Houthoofd, S. Kerkhofs, J.A. Martens, P.A. Jacobs, B.F. Sels, Ternary Ag/MgO-SiO_2 Catalysts for the Conversion

of Ethanol into Butadiene, ChemSusChem. 8 (2015) 994–1008. doi:10.1002/cssc.201402894.

[36] M. León, E. Díaz, S. Ordóñez, Ethanol catalytic condensation over Mg-Al mixed oxides derived from hydrotalcites, Catal. Today. 164 (2011) 436–442. doi:10.1016/j.cattod.2010.10.003.

[37] H. Niiyama, S. Morii, E. Echigoya, Butadiene Formation from Ethanol over Silica-Magnesia Catalysts, Bull. Chem. Soc. Jpn. 45 (1972) 655–659. doi:10.1246/bcsj.45.655.

[38] S. Da Ros, M.D. Jones, D. Mattia, M. Schwaab, F.B. Noronha, J.C. Pinto, Modelling the effects of reaction temperature and flow rate on the conversion of ethanol to 1,3-butadiene, Appl. Catal. A Gen. 530 (2017) 37–47. doi:10.1016/j.apcata.2016.11.008.

[39] Y. Xu, Z. Liu, Z. Han, M. Zhang, Ethanol/acetaldehyde conversion into butadiene over sol–gel ZrO_2–SiO_2 catalysts doped with ZnO, RSC Adv. 7 (2017) 7140–7149. doi:10.1039/C6RA25139K.

[40] P.T. Patil, D. Liu, Y. Liu, J. Chang, A. Borgna, Improving 1,3-butadiene yield by Cs promotion in ethanol conversion, Appl. Catal. A Gen. 543 (2017) 67–74. doi:10.1016/j.apcata.2017.05.025.

[41] J.L. Cheong, Y. Shao, S.J.R. Tan, X. Li, Y. Zhang, S.S. Lee, Highly Active and Selective Zr/MCF Catalyst for Production of 1,3-Butadiene from Ethanol in a Dual Fixed Bed Reactor System, ACS Sustain. Chem. Eng. 4 (2016) 4887–4894. doi:10.1021/acssuschemeng.6b01193.

[42] A. Talalay, L. Talalay, S.K.-The Russian Synthetic Rubber From Alcohol - A Survey of the Chemistry and Technology of the Lebedev Process for Producing Sodium-Butadiene Polymers, Rubber Chem. Technol. 15 (1942) 403–429.

http://rubberchemtechnol.org/doi/pdf/10.5254/1.3543128.

[43] Q. Zhu, B. Wang, T. Tan, Conversion of Ethanol and Acetaldehyde to Butadiene over MgO–SiO $_2$ Catalysts: Effect of Reaction Parameters and Interaction between MgO and SiO_2 on Catalytic Performance, ACS Sustain. Chem. Eng. 5 (2017) 722–733. doi:10.1021/acssuschemeng.6b02060.

[44] M. Zhang, X. Tan, T. Zhang, Z. Han, H. Jiang, The deactivation of a ZnO doped ZrO $_2$ – SiO $_2$ catalyst in the conversion of ethanol/acetaldehyde to 1,3-butadiene, RSC Adv. (2018). doi:10.1039/C8RA06757K.

[45] A.G. Panov, J.J. Fripiat, Poisoning of aldol condensation reaction with H2O on acid catalysts, 57 (1999) 25–32. doi:10.1023/a:1019079011862.

[46] I. Yasumoto, Adsorption of water, ammonia, and carbon dioxide on zinc oxide at elevated temperatures, J. Phys. Chem. 88 (1984) 4041–4044. doi:10.1021/j150662a036.

Supporting Information

for

Ethanol conversion into 1,3-butadiene over a mixed Hf-Zn catalyst: effect of reaction conditions and water content in ethanol

G. M. Cabello González[1], P. Concepción[2], A. L. Villanueva Perales*[1], A. Martínez[2], M. Campoy[1], F. Vidal-Barrero[1]

[1] Departamento de Ingeniería Química y Ambiental, Escuela Técnica Superior de Ingeniería, Universidad de Sevilla, Camino de los Descubrimientos, s/n. 41092 Sevilla, Spain.

[2] Instituto de Tecnología Química, Universitat Politècnica de València - Consejo Superior de Investigaciones Científicas (UPV-CSIC), Avda. de los Naranjos s/n, 46022 Valencia, Spain.

Table S1. Experimental results of the conversion of ethanol to 1,3-butadiene over the one-step mixed Hf-Zn catalyst at different reaction temperatures (T), space velocities (WHSV), and water contents in the ethanol feed.

T	Water	WHSV	TOS	X	Y_{BD}	Selectivity (%)						
(°C)	(wt%)	(h^{-1})	(h)	(%)	(%)	BD	ET	DEE	C4	AC	C_{6+}	Others
340	0	1.12	19	69.2	28.5	41.2	4.6	1.6	4.6	10.8	13.6	23.5
	0	3.2	15	52.9	23.3	44.1	3.8	1.6	3.8	23.2	6.9	16.6
	0	6.1	10	41.6	15.7	37.9	3.3	1.6	2.8	36.2	3.9	14.2
	0	9.8	5	32.9	10.7	32.8	3.3	1.7	2.3	43.6	4.1	12.1
	7.5	1.12	19	59.9	29.8	49.8	9.0	3.5	4.9	19.9	2.9	9.9
	7.5	3.2	15	45.8	17.7	38.7	6.3	2.8	2.8	40.0	2.6	6.8
	7.5	6.1	10	33.4	9.1	27.3	5.3	2.6	1.7	55.7	1.8	5.5
	7.5	8.0	4.5	25.4	5.8	23.1	5.1	2.5	1.4	61.5	1.6	4.7
	15	1.12	16	54.9	25.5	46.6	10.5	4.0	4.3	24.2	2.3	8.1
	15	3.2	11	35.2	11.7	33.5	7.4	3.3	2.2	47.2	1.2	5.2
	15	6.1	7	29.2	6.5	22.3	6.2	2.9	1.2	62.5	0.9	3.8
	15	8.0	4	24.6	4.9	20.0	6.0	2.8	1.2	65.3	1.1	3.6
360	0	1.12	22	87.1	39.3	45.1	5.6	1.1	5.6	9.6	13.3	19.6
	0	3.2	16	70.9	33.1	46.7	4.2	1.2	4.2	22.9	5.7	14.8
	0	6.1	11	60.4	25.5	42.3	3.7	1.2	3.5	28.1	5.6	15.5
	0	9.8	7	51.4	20.0	38.9	3.5	1.2	2.9	33.8	4.9	14.7
	3.75	1.12	23	82.2	41.2	50.2	9.2	2.2	5.3	15.5	3.3	14.4
	3.75	3.2	19	68.5	32.1	46.9	7.6	2.2	4.1	24.7	2.8	11.6
	3.75	6.1	12	48.4	18.9	39.3	5.8	2.1	2.6	3.0	2.3	45.0
	3.75	8.0	7	44.1	16.1	36.4	5.5	2.1	2.3	44.2	1.8	7.7
	7.5	1.12	26	78.0	38.3	49.1	9.5	2.3	5.3	16.6	3.9	13.2
	7.5	3.2	18	59.9	26.0	43.5	6.8	2.1	3.5	32.4	2.3	9.4
	7.5	6.1	13	48.6	17.6	36.3	5.6	2.0	2.5	43.5	1.8	8.3
	7.5	8.0	8	43.7	15.4	35.4	5.3	1.9	2.3	44.9	2.1	8.1
	15	1.12	27	79.1	37.4	47.3	11.4	2.6	5.1	18.4	3.3	11.9
	15	3.2	21	59.4	24.0	40.5	8.4	2.5	3.1	35.8	1.9	7.8
	15	6.1	14	45.8	14.4	31.5	6.9	2.5	2.0	49.8	1.2	6.1
	15	8.0	7	43.4	12.5	28.8	6.4	2.4	1.6	53.1	1.7	5.9
380	0	1.12	23	95.2	27.4	28.7	3.4	0.5	2.9	9.2	34.2	23.0
	0	3.2	18	90.0	30.8	34.2	3.5	0.5	3.4	15.3	21.9	21.1
	0	6.1	12	77.4	32.3	41.8	4.3	0.9	3.8	24.6	7.9	16.6
	0	9.8	7	66.7	28.6	42.9	4.5	1.1	3.6	28.3	5.7	13.9
	7.5	1.12	22	96.5	48.0	49.7	8.7	1.3	5.4	11.6	8.4	14.8
	7.5	3.2	18	85.0	39.3	46.2	7.3	1.3	4.1	26.2	2.7	12.2
	7.5	6.1	12	72.3	30.7	42.4	6.4	1.6	3.2	34.2	2.2	10.0
	7.5	8.0	6	65.0	26.6	40.9	6.1	1.7	2.8	36.5	2.3	9.7
	15	1.12	18	98.1	45.4	46.3	10.3	1.4	5.1	15.4	6.9	14.6
	15	3.2	14	84.4	38.8	45.9	8.6	1.5	3.8	27.1	2.5	10.5
	15	6.1	8	69.0	27.4	39.7	7.1	1.7	2.8	37.9	2.5	8.3
	15	8.0	5	64.7	25.5	39.4	6.9	1.8	2.5	38.7	2.5	8.2

Note: TOS= time on stream, X= ethanol conversion, Y= yield, BD= butadiene; ET=ethene; DEE=diethyl ether; C4= butenes; AC=Acetaldehyde; C_{6+}= heavy compounds. "Others" comprises a mixture of minor sub-products such as acetone, ethyl acetate, butanal, butanol, 2-ethyl-hexenal, CO, CO_2 and CH_4.

Figure S1. IR spectra in the νOH region of pre-activated a) hemimorphite (HM), b) Hf/SiO_2, and c) $HfZn/SiO_2$.

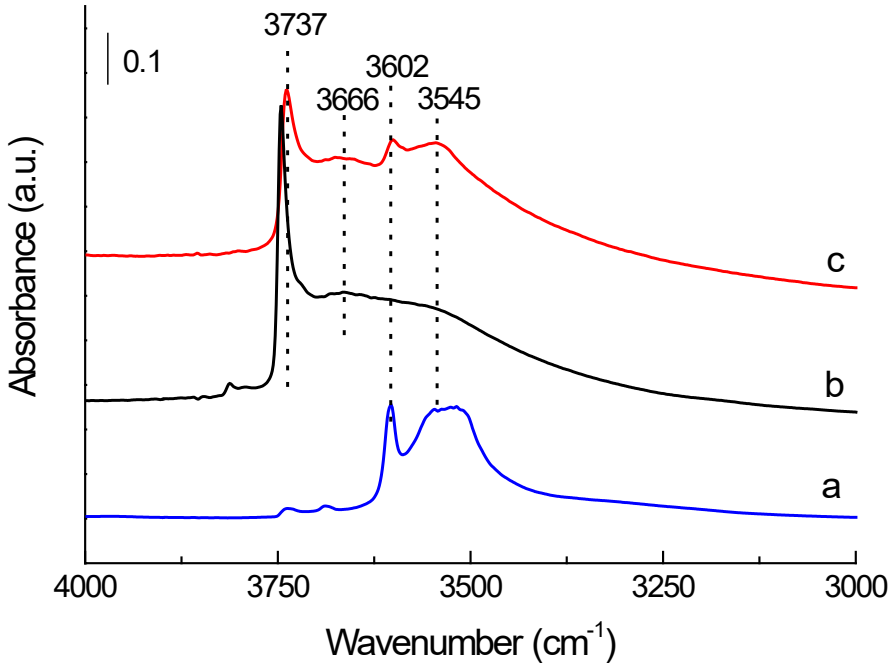

Figure S2. Parity plots of the experimental data used in the regression and the model predictions, featuring bands for relative error of 10 and 20%.

a)

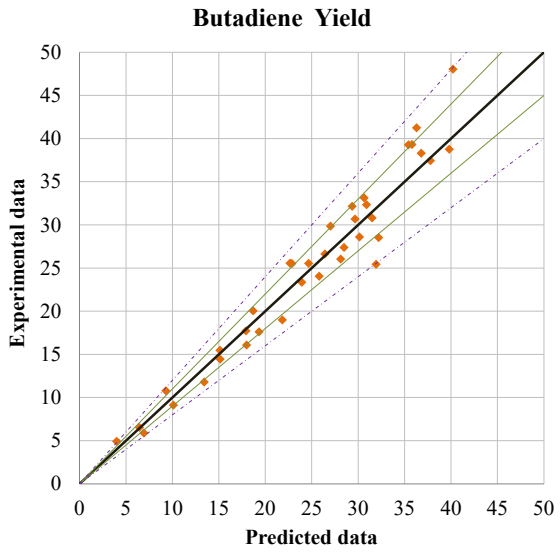

b)

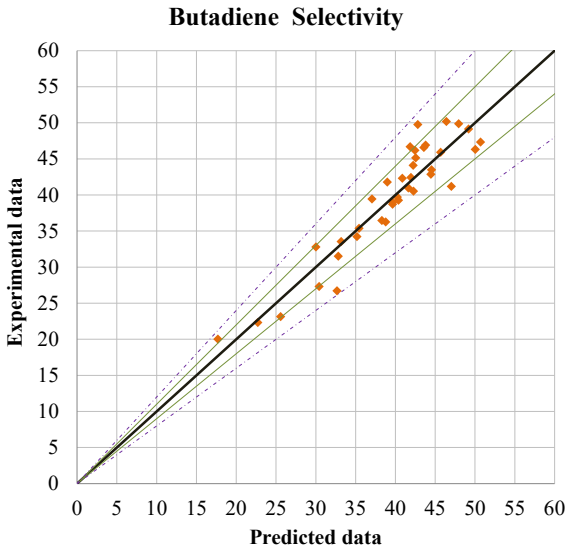

c)

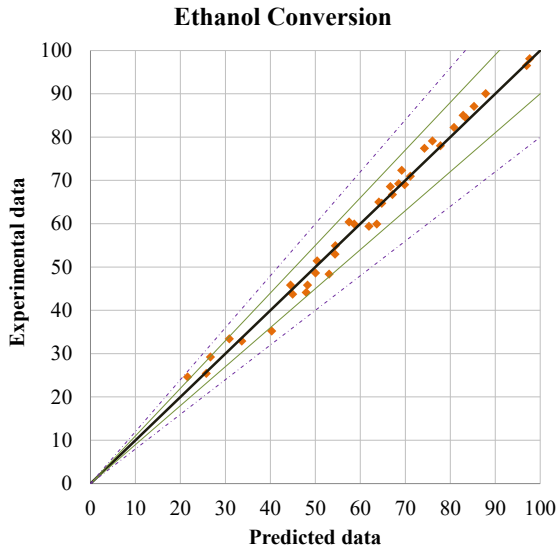

d)

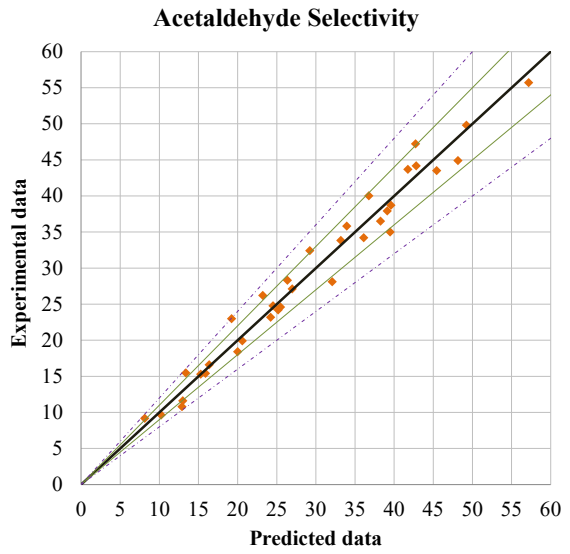

e)

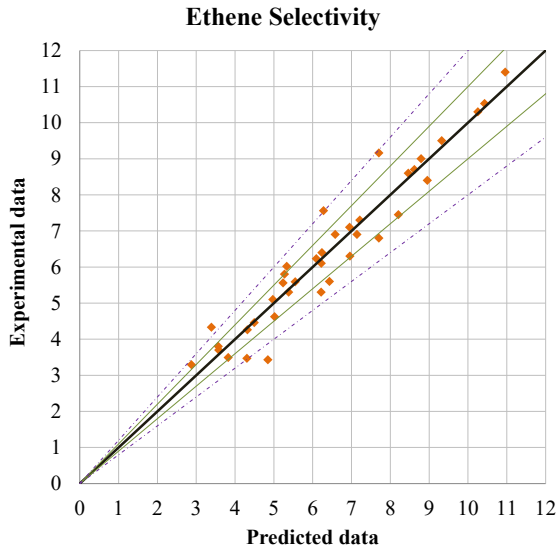
Ethene Selectivity
Experimental data
Predicted data
0 1 2 3 4 5 6 7 8 9 10 11 12

f)

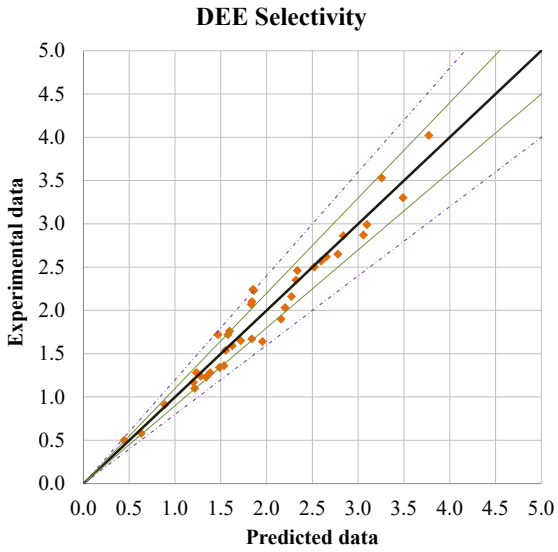
DEE Selectivity
Experimental data
Predicted data
0.0 0.5 1.0 1.5 2.0 2.5 3.0 3.5 4.0 4.5 5.0

g)

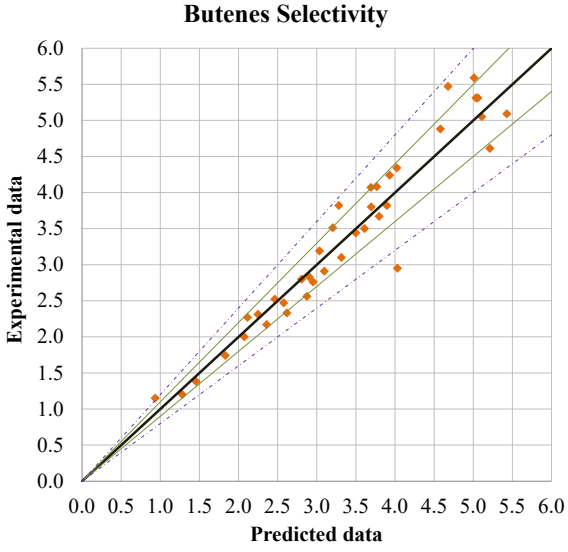
Butenes Selectivity
Experimental data
Predicted data
0.0 0.5 1.0 1.5 2.0 2.5 3.0 3.5 4.0 4.5 5.0 5.5 6.0

h)

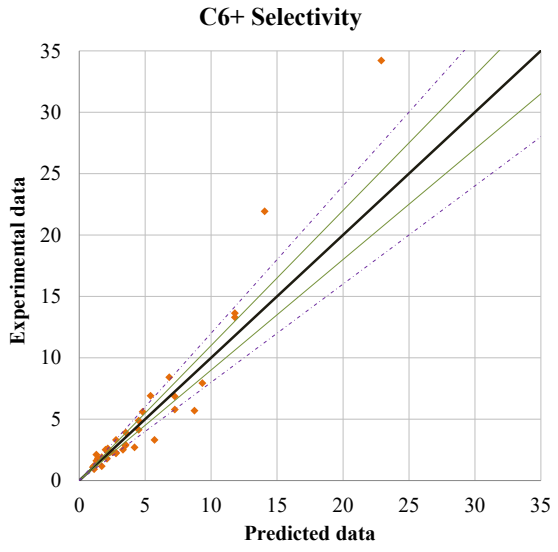
C6+ Selectivity
Experimental data
Predicted data
0 5 10 15 20 25 30 35

Figure S3. Effect of water content in the yield to butenes at 360 °C (left panel) and 380 °C (right panel) as a function of space velocity and water content (wt%) in ethanol.

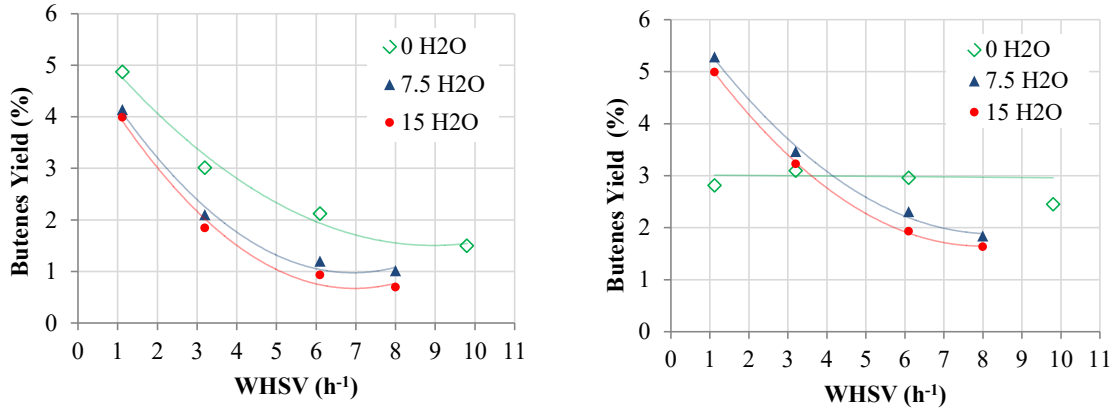

Figure S4. Comparison of catalyst deactivation in the absence and presence of water in the ethanol feed. Operating conditions: T = 360 °C, partial pressure of ethanol 0.21 bar, and total pressure 1 bar. The space velocity for the experiment feeding ethanol with 7.5 wt% water (WHSV=0.4 h^{-1}) was adjusted to nearly match the initial ethanol conversion (~90%) for the experiment with anhydrous ethanol (WHSV=1.12 h^{-1}).

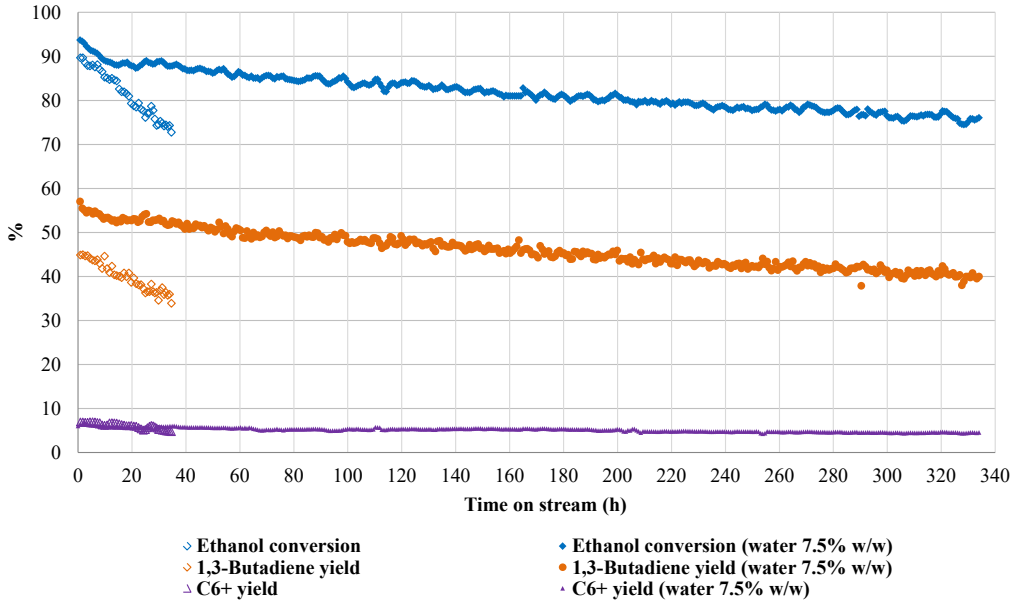

As seen in the figure, the time on stream at which the catalyst losses 20 percentage points of its initial conversion remarkably increases from ~40 h in absence of water to ~340 h in presence of water, implying an 8.5-fold reduction in the catalyst deactivation rate when feeding hydrous (7.5 wt% water) ethanol.